Applied Surface Science 257 (2011) 8634–8639

Contents lists available at ScienceDirect

Applied Surface Science

journal homepage: www.elsevier.com/locate/apsusc

Effect of temperature and pumping power on the photoluminescence properties of type-II CdTe/CdSe core-shell QDs

A.M. Saad, M.M. Bakr, I.M. Azzouz, Maram T.H. Abou Kana *

National Institute of Laser Enhanced Science, Cairo University, Giza 12613, Egypt

ARTICLE INFO

Article history:
Received 29 September 2010
Received in revised form 6 May 2011
Accepted 9 May 2011
Available online 14 May 2011

Keywords:
CdTe-CdSe core-shell
Near IR-spectrum
Photoluminescence
Quantum dots
Lifetime

ABSTRACT

CdTe/CdSe core-shell QDs type II was prepared by two steps synthetic process and embedded in polymer host. Emission in the NIR region was recorded. The effect of Ar laser excitation at different powers on the optical properties of the prepared QDs is studied at different temperatures (300–10 K). Amplified spontaneous emission is observed at room temperature and at 10 K. Also, lifetime measurement of prepared QDs was documented using N_2-laser.

1. Introduction

Semiconductor nanocrystals have received considerable attention since the last two decades due to their unique optical, optoelectronics, magnetic and electrical properties that are different from their bulk structure counterpart [1]. The binary systems of semiconductors quantum dots (QDs), such as CdTe and CdSe, have been synthesized and used as active agent because of their rich luminescent properties with unique tunable, narrow emission spectrum and high-quantum yield photoluminescence [2–5] characteristics. These characteristics are interesting in light emitting diodes [6], lasers [4], and biomedical tags for fluoroimmunoassays, nano-sensors, and biomedical imaging in living tissue by taking advantage of their great photostability and deeper light penetration [7,8] and LED application [9,10,1,11,12].

To realize this wide range of potential applications, the luminescent properties (emission color, photoluminescence quantum yield (PL QY), luminescence lifetime, and stability) of semiconductor NCs must be strictly controlled. At present, the control and reproducibility of the PL QY has remained an elusive issue, only recently some of the factors determining the PL efficiency of NCs have been properly addressed [13–15]. On the other hand, the QDs must suppress the non-radiation recombination on the surface and improve the confining potential. One of the ways to achieve this condition is by capping the core-QDs with inorganic material as a shell with higher energy gap. The electrons and holes are expected to be fully trapped inside the core. This may also effectively suppress the nonradiative recombination of electrons and holes on the QDs surface due to the pressure of shell materials [16]. Hence the quantum yield could be increased.

Core-shell QDs are divided into type-I and type-II like bulk semiconductors, depending on their band gap structure. In the type-I structures, both the conduction and the valence band edges of core semiconductor QDs are located within the energy gap of the shell semiconductor QDs. In this case, an electron–hole (e–h) pair excited near the interface tends to localize in core, which provides the lowest energy states for both electron and hole [17,18]. This approach allows one to reduce interactions of core-localized e–h pairs (excitons) with surface traps, which can result in significant improvements in NC emission quantum yields (QYs) [19,20].

Type-II core-shell QDs have staggered band offsets, namely, a higher valence band or lower conduction band in the shell than in the core. As a result, the wave functions of the electron and hole exist separately, which leads to many novel properties, for example, the red shift of the emission and a long decay lifetime [21]. Interesting opportunities are associated with the use of the type-II regime in colloidal structures which could allow, for example, control of both single [22] and multiexciton [23] lifetimes. Furthermore, spatial separation between positive and negative charges produced in these structures can simplify applications of NCs in photovoltaic technologies. Additionally, since the band-edge transition energy in the type-II structure is smaller than the energy gap of either material comprising it, the type-II hetero-NCs can be used, e.g., in obtaining infrared emission wavelengths using

* Corresponding author.
E-mail address: mabou202@niles.edu.eg (M.T.H. Abou Kana).

0169-4332/$ – see front matter © 2011 Elsevier B.V. All rights reserved.
doi:10.1016/j.apsusc.2011.05.040

combinations of well-studied wide-gap semiconductors [24]. Finally, one potentially important application of type-II structures is in NC lasing technologies, where they can be utilized for obtaining optical gain in the low-threshold single-exciton regime [19] without complications associated with multiexciton nonradiative Auger recombination [25].

In this paper CdTe/CdSe core-shell QDs was prepared and embedded in polymeric host. The optical properties of the prepared samples was investigated at different pumping powers of Ar-laser (1–200 mW). This investigation was carried out at different temperatures (300–10 K). The prepared samples yielded emission in the NIR region. Amplified stimulated emission is observed at room temperature and at 10 K. Also, lifetime measurement was carried out using N_2-laser.

2. Experiment

2.1. Materials

Cadmium oxide {(CdO), Fluka, 99%}, Selenium powder {(Se), Riedel, 99%}, Trioctyl phosphine {(TOP), Fluka, 90%}, Hexadecyl amine {(HDA), Aldrich 97%}, Trioctylphosphine oxide {(TOPO), Fluka 97%}, Oleic acid {(OA), ($C_{70}H_{33}COOH$), Qualikems 98%}, Sodium borohydride {$NaBH_4$, Aldrich 95%}, Sodium hydroxide {NaOH}, 2,2′-Azobis(2-methylpropionitrile) {Aldrich 98%}, Methyl methacrylate {(MMA, Merck 99%)}, Thioglycolic acid {(TGA), $HSCH_2COOH$, SDS 80%}, Toluene {C_7H_8 ($C_6H_5CH_3$), Riedel 99.5%}, Methanol {CH_3OH, Sigma–Aldrich 99.9%}, Acetone {C_3H_6O, SDS 99.8%}.

2.2. Preparation of CdTe/CdSe core-shell quantum dots

CdTe/CdSe core/shell QDs type-II was prepared by a two-step synthetic process. 0.2 g of CdTe nanocrystals – prepared via Peng et al. [26] procedure – were dissolved in 5 ml toluene then added to a mixture of 1 g of TOPO and 1 g of HAD. The reaction mixture was heated up to 150 °C. Cd element was prepared by dissolving 0.1 g of CdO in 3 ml of oleic acid at 180 °C. as the same time, 0.1 g of Se powder was dissolved in 3 ml of TOP. Both clear monomers were obtained under the flow of Ar gas. Then, allowed to cool to room temperature. Equal volumes of Cd and Se elements were mixed for preparing Cd–Se injection solution and added drop-wise (using a syringe at a rate of 5 drops/min) to the vigorously stirred CdTe core solution at 150 °C. After complete addition, the reaction mixture was allowed to cool down to room temperature. Finally, the CdTe/CdSe core/shell type-II QDs were precipitated by the addition of acetone, then separated, and finally re-dispersed for further processing.

2.3. Embedding nanocrystals in polymer matrix

To embed the prepared CdTe/CdSe core-shell NCs in a polymeric host, 0.1 ml solution of CdTe/CdSe core-shell was added to 2 ml of freshly purified MMA monomer. Then, the required amount of 2,2′-azo-bis(isobutyronitrile) (AIBN) used as a thermal free radical initiator was added and allowed to dissolve in a ultrasonic bath for about 5 min. The resulting solution was filtered into soda glass tube (2.2 cm diameter and 20 cm length). After careful deaeration by purging with inert gas (argon gas), the test tube was sealed. Copolymerization reaction was performed at 60 °C in absence of light for 3 days.

2.4. Instrumentation

Absorption spectra were recorded with a Perkin Elmer Lambda 35 spectrometer. Fluorescence emission and excitation spectra were measured using Perkin Elmer LS55.

LIF technique is used to measure the fluorescence of the prepared quantum dot samples for studying the electronic structure of molecules and their interactions at low and at different range of temperatures. A schematic diagram of the experimental setup is shown in Fig. 1. Ar ion laser (Lexel Model 95) of wavelength 488 nm was focused by lens to excite the samples at different values of power ranges from 1 to 200 mW (using a filter power density). The emitted light from the samples was collected and focused on a monochrometor through a filter to avoid scattering. The effect of exciton and biexcitonic states in semiconductor quantum dots could be observed by studying the photoluminescence properties at different excitation powers and at different temperatures. The temperature of the samples could be controlled using a liquid helium path cryostat (CTI-CRYOGENICS), with an electrical heater (Scientific Instrument Inc. 9620-1). The fluorescence measurements were carried out at different temperature values of the quantum dots (ranges from 8 to 300 K). The output signal (PL signal) was collected at the slit of the monochromator [SPEX 750 M] with a grating (1200 g/mm). The resolution of the monochromat is 1 Å.

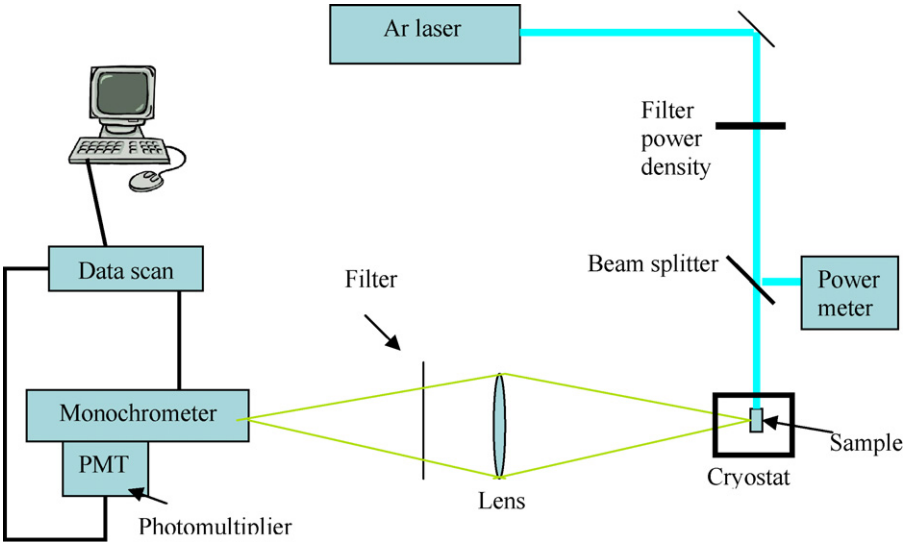

Fig. 1. Laser induced florescence (LIF) with cooling system.

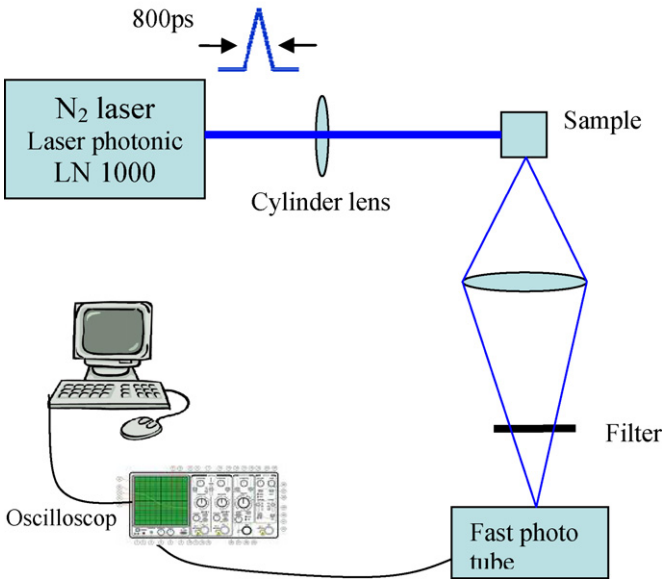

Fig. 2. Lifetime measurement system at room temperature.

The monochromator is connected to Data scan (SPEX DS1010). The monochromator was synchronized and amplified with the photomultiplier.

The lifetime was measured using nitrogen laser (laser photonics LN1000) of pulse duration of 800 ps and wavelength 337 nm. The maximum energy per pulse was 2 mJ. A schematic diagram of the optical experimental setup for measuring the lifetime and the relaxation dynamics of QDs is shown in Fig. 2. The beam of N_2 laser was focused by a cylindrical lens onto the sample. The sample's emission was detected using a fast phototube (Hamamatsu R1328U) then displayed and measured on the oscilloscope (EZ Wide View DS 1530/300 MHz).

3. Results

The absorption and emission spectra of the QDs: CdTe, CdSe and CdTe/CdSe core/shell are presented in Fig. 3(a). A red shift of nearly ~20 nm is observed in the emission spectra of each of CdTe and CdSe QDs relative to their absorption. However, in case of CdTe/CdSe core-shell QDs, the red shift is increased to be about ~220 nm yielding an emission in the NIR region. This large stock shift was attributed to the formation of CdTe/CdSe hetrostructure core/shell of type II (Fig. 3(b)). Type II core-shell allows for radiative recombination of electrons reside in the lower conduction band of CdSe shell with holes confined in the higher valence band of CdTe core. Re-absorption process was expected to be reduced due to the large stock shift [17,18,24–26]. The emission spectrum of CdTe/CdSe QDs is observed at longer wavelengths than that of the corresponding cores. Type-II emission is the "deep trap" luminescence often observed in cores [19,27]. It originates from the radiative recombination of the electron-hole pair across the core-shell interface. The energy of the emission thus depends on the band offsets of the two materials (the core and the shell) and can emit at energies smaller than the band gap of either material [19,27,28]. Therefore, formation of type II CdTe/CdSe core-shell QDs can tune the band gap from visible to NIR region depending on the thickness of the shell and the size of the core.

To compare the absolute emission intensity of CdTe QD's and CdTe/CdSe core-shell QD's, photoluminescence quantum yield measurements have been carried out. The results are presented in Fig. 3(c). These measurements have been carried out using ethanolic solution of R6G dye as a reference. The quantum yield of CdTe QD's sample was very small (does not exceed 3%) compared to CdTe/CdSe core-shell QD's sample which yield over 40%. This behavior was observed before [28] and was attributed to the enhancement in the radiative recombination due to decrease the defects at the interface of CdTe/CdSe core-shell (inorganic–inorganic interfaces) than the interface of CdTe QD's with organic material (inorganic–organic interface). [28].

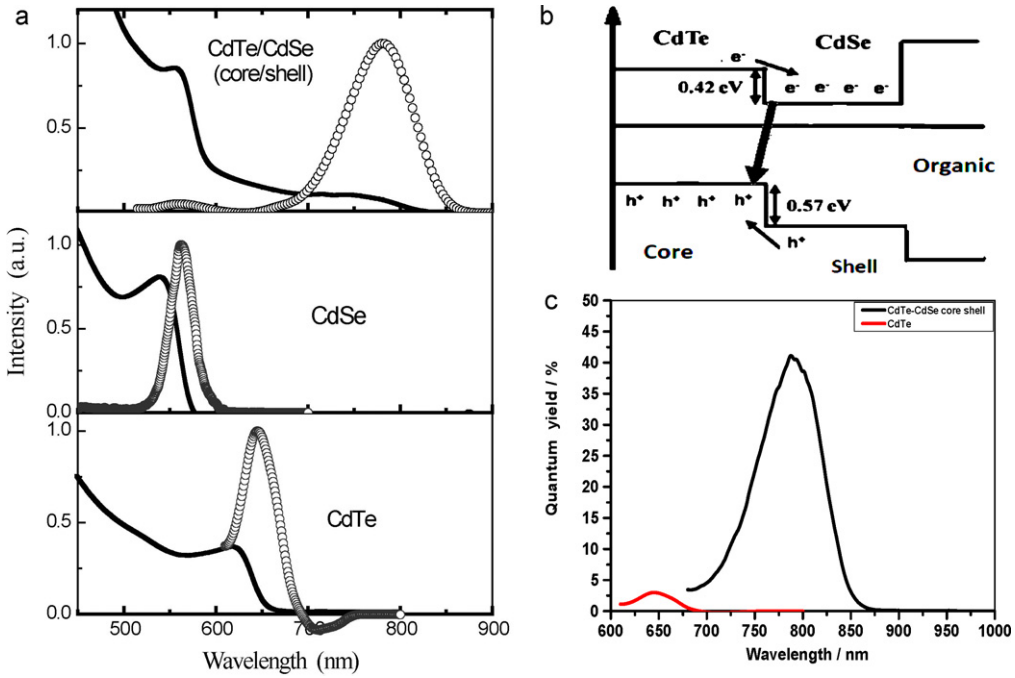

Fig. 3. (a) Absorbance and normalized emission of QDs: CdTe, CdSe and CdTe/CdSe core/shell. (b) Schematic diagrams of type II band alignment. (c) Quantum yield of CdTe (red) QD's and CdTe-CdSe (black) core-shell QD's. (For interpretation of the references to color in this figure legend, the reader is referred to the web version of the article.)

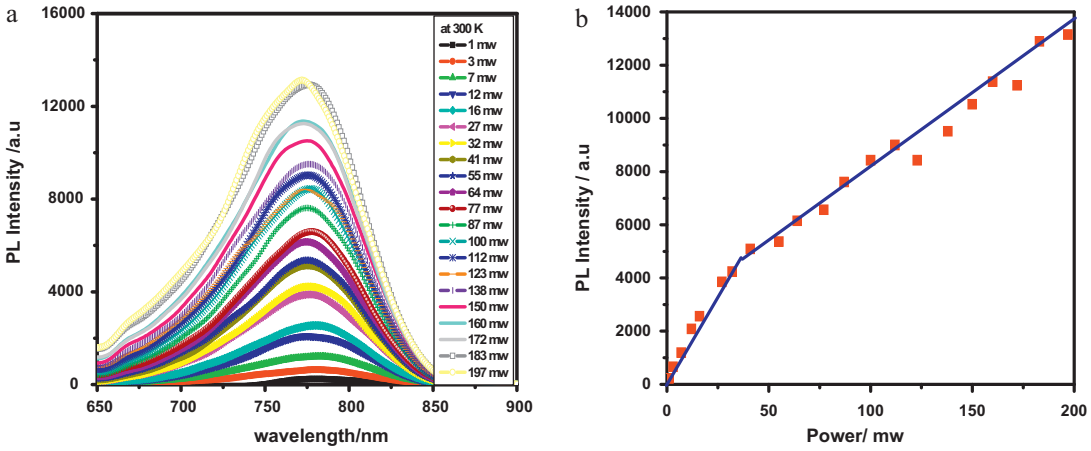

Fig. 4. (a) The emission spectra of CdTe/CdSe core-shell nanoparticle at different laser excitation power at room temperature. (b) The relation between the excitation power and the intensity of the emission spectra which shows linear relation with two different slopes.

LIF technique is used to monitor the effect of laser excitation power on the emission spectra of CdTe/CdSe core-shell quantum dots. This is examined at room temperature and at low temperature (10 K).

At room temperature, the changing in the emission properties of core-shell CdTe/CdSe by increasing the excitation power as shown in Fig. 4. The sample of fixed concentration has been excited by 488 nm of Ar-laser with different excitation power ranging from 2 to 200 mW.

The amplitude of emission band increases linearly with increasing the excitation density up to 35 mW. This linear relation indicates the formation of the monoexciton. At higher excitation powers (>35 mW), the emission intensity also increased but with different slope. This indicates a population of another state or the formation of another species.

The effect of excitation power on the emission spectra is shown in Fig. 5. The blue shift by 11 nm (~21 meV) is observed in the normalized emissions due to excitation by high and low powers (200 and 3 mW, respectively). This means that at low pump power, only monoexciton state is existed but at higher pumping power, a new species is formed.

Troparevsky [29] studied the monoexciton X (one electron, one hole, 1e–1h), the charged excitons X^- (2e–1h) and X^+ (1e–2h), and the charged biexcitons XX^- (3e–2h) and XX^+ (2e–3h). He found that the lowest energy emission peak for the X^- recombination is slightly red shifted (by 5 meV) with respect to the monoexciton, while the X^+ emission peak is blue shifted by 15 meV. We also found that the main emission peaks from the XX^- and XX^+ recombination are blue shifted by 70 and 89 meV, respectively, with respect to the single exciton X. Thus, the blue shift in Fig. 5 and the change in the slope in Fig. 4 are indication for the formation of a state similar to positive trion (X^+) with excitation power >35 mW at room temperature.

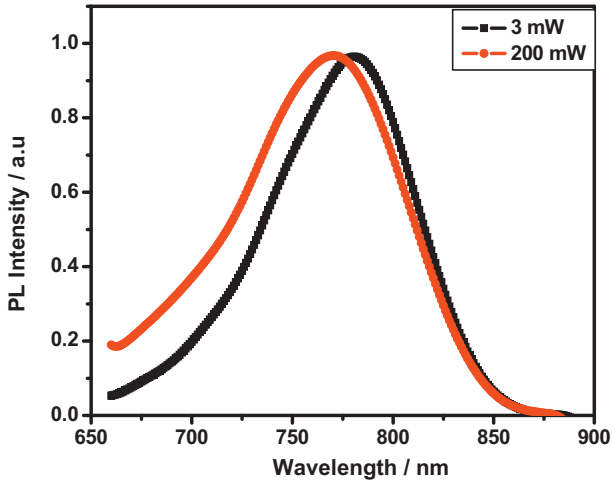

Fig. 5. Normalized emission spectrum of CdTe/CdSe core-shell nanocrystals at room temperature at low power (black) and high laser excitation power (gray). The emission band is shifted to the blue side of about 11 nm, and the band became slightly broader (difference of brooding ~12 nm at FWHM).

At low temperature, the nanocrystals of CdTe/CdSe core-shell were embedded in polymer in order to form elastic transparent polymeric film at low temperature. Fig. 6 shows the effect of different temperatures on the emission spectra of CdTe/CdSe core-shell QDs sample ranging from room temperature (300 K) to very low temperature (10 K). With different excitation power, the following have been observed: (a) at low excitation power, the emission maxima shifts to higher energies (~13 nm) with decreasing temperature, and the broadening of the emission spectra also decease at FWHM (~11 nm). (b) At high excitation power, blue shift occurs in the emission peak with decreasing temperature (~8 nm) and narrowing in broadening at FWHM (~17 nm).

The blue shift and reduction in the FWHM at low temperature does not depend on the excitation power. This indicates that, there is no contribution from thermal processes such as Auger ionization, surface trapping, and phonon contribution.

Scince these effects are eliminated at low temperature, thus, all the absorbed photons by the samples generate e–h pairs which relax by radiative recombination. It is clear from Fig. 7 that the emission intensity enhanced greatly by increasing the excitation power at low temperature. The relation between the power and the emission intensity shows linear increase due to the formation of the monoexciton (X), then break at 70 mW and saturation occurred between 70 and 150 mW and again linear increase but with different slope. This indicates that after the break, another state or specie is formed. At the saturation region (between 70 and 150 mW) biexciton is formed in core and monoexciton in shell. So two holes are in V.B of core and one electron is in C.B of shell. One electron in C.B of shell are recombining with one hole in V.B in core and emitting photon (radiative recombination). Excess of holes in V.B of core or shell are recombining with excess of electrons in C.B in core or shell and emitting phonon (nonraditive recombination by auger process) as shown in Fig. 8. This explains the saturation region with increase power between 70 and 150 mW. In Fig. 7(b), while the pumping power become more than 150 mW, the emission intensity increases linearly again with higher slope than in

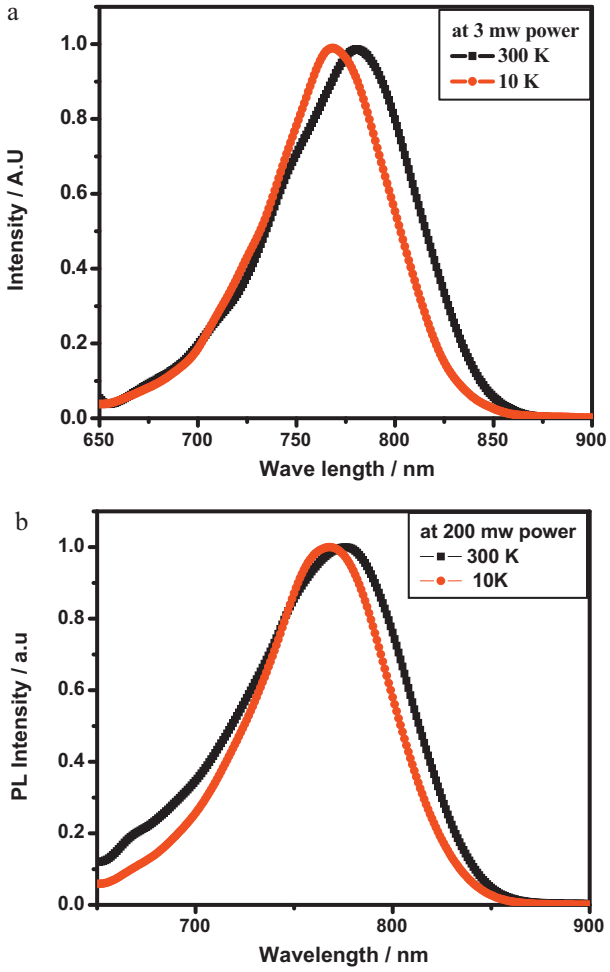

Fig. 6. Normalized emission spectrum of CdTe/CdSe core-shell nanocrystals at room temperature (black) and at 10 K (red): (a) comparing the emission spectra at different temperatures and using low laser excitation power, (b) at high excitation power. (For interpretation of the references to color in this figure legend, the reader is referred to the web version of the article.)

beginning. This is an indication for the biexciton (XX) formation of in each of the core and the shell. Then, radiative recombination is takes place between two electrons in C.B of shell and two holes in V.B of core emitting 2 photons. Also we note in Fig. 7(b) that the threshold power of stimulated emission at which biexciton is

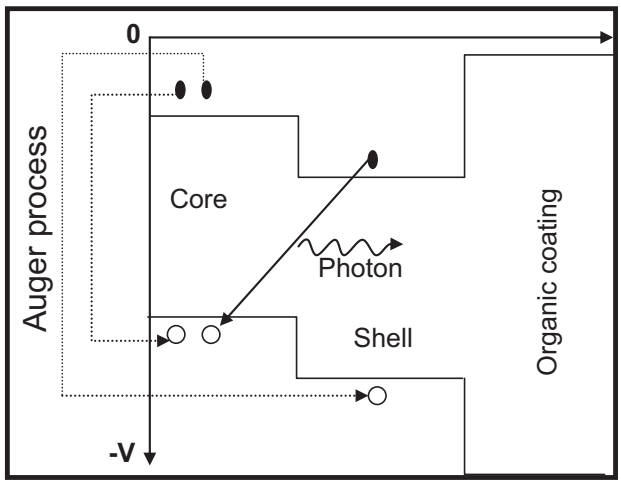

Fig. 8. Radiative and nonradiative emitting in CdTe/CdSe core-shell NCs at saturation region (70–150 mW).

formed in CdTe/CdSe core-shell NCs is 77 mW which depend on the size of the core and thickness of the shell.

In Fig. 9 we note an emission blue shift of 3 nm between higher excitation power (200 mW) and lower excitation power (3 mW). Also, the FWHM is increased by 5 nm with increasing pumping power. It means that, at low pumping power the monoexciton state is present but and at higher power biexciton state is formed.

The lifetime of CdTe/CdSe core-shell samples was measured at room temperature using nitrogen laser of 800 ps pulse duration and 337 nm wavelength and the energy was 0.5 mJ/pulse. The lifetime is expected to be overlapped between monoexciton (X) and biexciton (XX) lifetimes. So a decay curve fitting was calculated using Origin Lab vr 8 which using a second order exponential decay with offset fitting equation:

$$y = y_0 + A_1 \exp\left(\frac{-(x - x_0)}{t_1}\right) + A_2 \exp\left(\frac{-(x - x_0)}{t_2}\right)$$

where y is PL intensity, y_0 is offset, x_0 is center, A_1 and A_2 are amplitudes of first and second decay, and t_1 and t_2 are lifetime of first and second decay. The lifetime of monoexciton and biexciton was found to be 7 and 2 ns (Fig. 10).

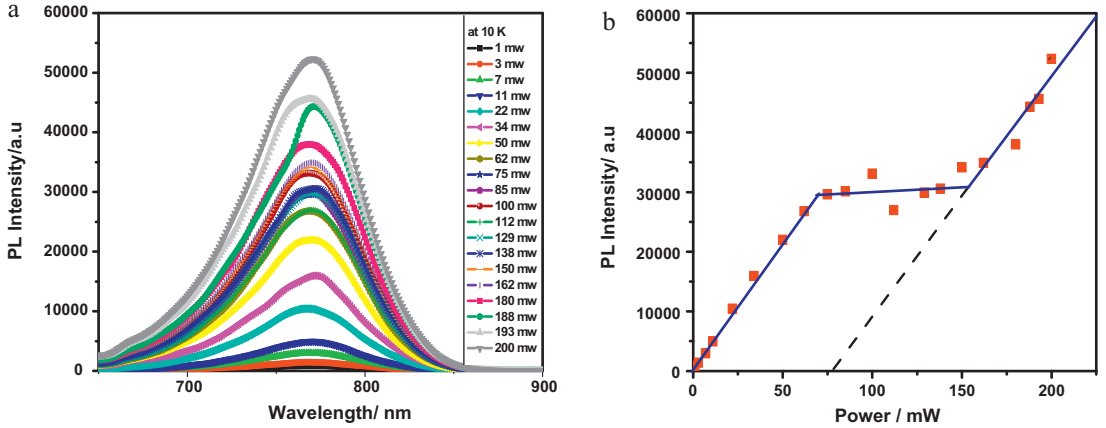

Fig. 7. (a) The emission spectra of CdTe/CdSe core-shell nanoparticle at different laser excitation power at low temperature. (b) The relation between the excitation power and the intensity of the emissions. Spectra show linear relation with three different slopes. Threshold power of biexciton (XX) state emission is 77 mW.

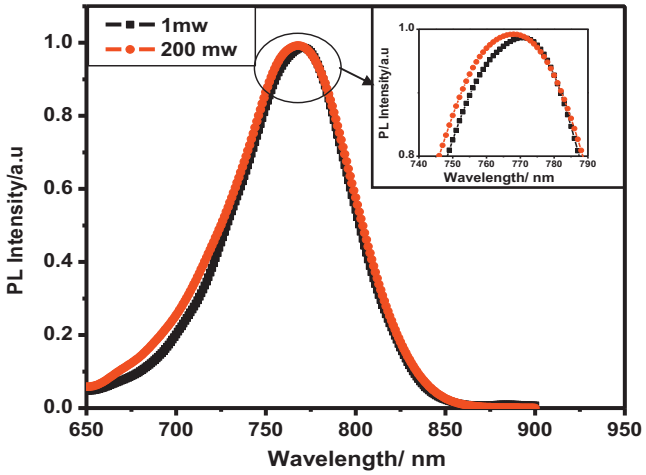

Fig. 9. Normalized emission spectrum of CdTe/CdSe core-shell nanocrystals at 10 K for low power (black) and high laser excitation power (red). The emission band is shifted to the blue side of about 3 nm, and the band became slightly broader (difference of brooding ~5 nm at FWHM).

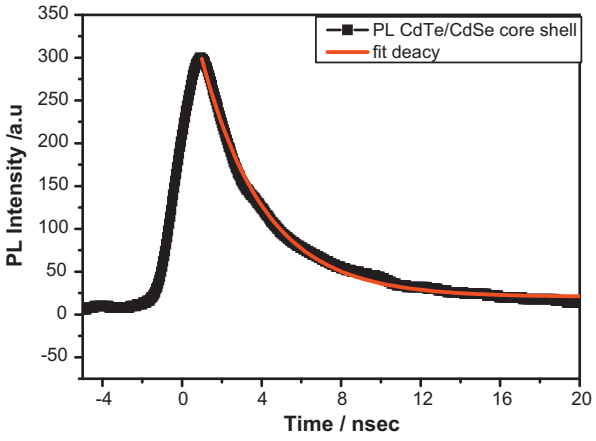

Fig. 10. Kinetics decay of the CdTe/CdSe core-shell nanocrystals excited by 0.5 mJ/pulse.

Acknowledgement

This work was supported by Semiconductor Lab. in the National Institute of Laser Enhanced Science (NILES), Cairo University, Egypt.

References

[1] N. Abu Bakar, A.A. Umar, M.M. Salleh, M. Yahaya, Synthesis of CdSe quantum dots: effect of surfactant on the photoluminescence property, Sains Malaysiana 39 (2010) 473–477.
[2] N. Abu Bakar, A.A. Umar, T.H. Tengku Aziz, S.H. Abdullah, M. Mat Salleh, M. Yahaya, B.Y. Majlis, Synthesis of CdSe quantum dots: effect of surfactant on the photoluminescence property, IEEE-ICSE Proc. (2008) 494–497.
[3] J.M. Klostranec, W.C.W. Chan, Quantum dots in biological & biomedical research: recent progress and present challenges, Adv. Mater. 18 (2006) 1953–1964.
[4] V.I. Klimov, A.A. Mikhailovsky, S. Xu, A. Malko, J.A. Hollingsworth, C.A. Leatherdale, Optical gain & stimulated emission in nanocrystal quantum dots, Science 290 (2000) 314–317.
[5] C. Wang, M. Sim, P. Guyo-Sionnest, Electrochromic nano-crystal quantum dots, Science 291 (2001) 2390–2392.
[6] M. Gao, C. Lesser, S. Kristein, H. Mohwald, A.L. Rogach, H. Weller, Electroluminescence of different colors from polycation/CdTe nanocrystal self-assembled films, J. Appl. Phys. 87 (2000) 2297–2302.
[7] D. Gerion, F. Pinaud, S.C. Williams, W.J. Warak, D. Zanchet, S. Weiss, A.P. livisatos, Synthesis and properties of biocompatible water-soluble silica-coated CdSe/ZnS semiconductor quantum dots, J. Phys. Chem. B 105 (2001) 8861–8871.
[8] S. Kim, Y.T. Lim, E.G. Soltesz, A.M. De Grand, J. Lee, A. Nakayama, J.A. Parker, T. Mihaljevic, R.G. Laurence, D.M. Dor, L.H. Cohn, M.G. Bawendi, J.V. Frangioni, Near-infrared fluorescent type II quantum dots for sentinel lymph node mapping, Nat. Biotechnol. 22 (2004) 93–97.
[9] S. Sepeai, A.A. Umar, M. Mat Salleh, M. Yahaya, Fabrication of CdSe quantum dots-PHF organic hybrid light emitting diode, IEEE-ICSE Proc. (2008) 228–231.
[10] T.H. Tengku Aziz, A.A. Umar, M. Mat Salleh, M. Yahaya, Electroluminescent from hybrid of CdSe quantum dots-organic light emitting diode, IEEE-ICSE Proc. (2008) 282–285.
[11] P.A. Lodahl, F.V. Driel, I.S. Nikolaev, A. Irman, K. Overgaag, D. Vanmaekelbergh, W.L. Vos, Controlling the dynamics of spontaneous emission from quantum dot by photonic crystals, Nature 30 (2004) 654–657.
[12] D.J. Miliron, S.M. Hughes, Y. Cui, L. Manna, J. Li, L. Wang, A.P. Alivisatos, Colloidal nanocrystal heterostructures with linear & branched topology, Nature 430 (2004) 190–195.
[13] L. Qu, X. Peng, Control of photoluminescence properties of CdSe nanocrystals in growth, J. Am. Chem. Soc. 124 (2002) 2049–2055.
[14] D.V. Talapin, A.L. Rogach, E.V. Shevchenko, A. Kornowski, M. Haase, H. Weller, Dynamic distribution of growth rates within the ensembles of colloidal II–VI and III–V semiconductor nanocrystals as a factor governing their photoluminescence efficiency, J. Am. Chem. Soc. 124 (2002) 5782–5790.
[15] Y. Ebenstein, T. Mokari, U. Banin, Fluorescence quantum yield of CdSe/ZnS nanocrystals investigated by correlated atomic-force and single-particle fluorescence microscopy, Appl. Phys. Lett. 80 (2002) 4033–4035.
[16] J.S. Steckel, J.P. Zimmer, S.N. Coe-Sullivan, E. Stott, V. Bulovic, M.G. Bawendi, Blue luminescence from (CdS)ZnS core-shell nanocrystals, Angew. Chem. Int. Ed. 43 (2004) 2154–2158.
[17] V. Yu. Vandyshev, V.S. Dneprovskii, V.I. Klimov, D.K. Korokov, Lasing on a transition between quantum-well levels in a quantum dot, JETP Lett. 54 (1991) 442.
[18] N.N. Ledentsov, V.M. Ustinov, A.Y. Egorov, A.E. Zhukov, M.V. Maksimov, I.G. Tabatadze, P.S. Koplev, Optical properties of heterostructures with InGaAs–GaAs quantum clusters, Semiconductors 28 (8) (1994) 832.
[19] S.A. Ivanov, J. Nanda, A. Piryatinski, M. Achermann, L.P. Balet, I.V. Bezel, P.O. Anikeeva, S. Tretiak, V.I. Klimov, Light amplification using inverted core/shell nanocrystals: towards lasing in the single-exciton regime, J. Phys. Chem. B 108 (2004) 10625.
[20] A.A. Mikhailovsky, A.V. Malko, J.A. Hollingsworth, M.G. Bawendi, V.I. Klimov, Multiparticle interactions and stimulated emission in chemically synthesized quantum dots, Appl. Phys. Lett. 80 (2002) 2380.
[21] V.I. Klimov, A.A. Mikhailovsky, S. Xu, A. Malko, J.A. Hollingsworth, C.A. Leatherdale, H.-J. Eisler, M.G. Bawendi, Optical gain and stimulated emission in nanocrystal quantum dots, Science 290 (2000) 314.
[22] R.D. Schaller, M.A. Petruska, V.I. Klimov, Tunable near-infrared optical gain and amplified spontaneous emission using PbSe nanocrystals, J. Phys. Chem. B 107 (2003) 13765.
[23] H. Htoon, J.A. Hollingsworth, R. Dickerson, V.I. Klimov, Giant optical activity in quasi-two-dimensional planar nanostructures, Phys. Rev. Lett. 91 (2003) 227401.
[24] Y. Cao, U. Banin, Growth and properties of semiconductor core/shell nanocrystals with InAs cores, J. Am. Chem. Soc. 122 (2000) 9692.
[25] V.I. Klimov, A.A. Mikhailovsky, D.W. McBranch, C.A. Leatherdale, M.G. Bawendi, Quantization of multiparticle Auger rates in semiconductor quantum dots, Science 287 (2000) 1011.
[26] C.H. Henry, D.V. Lang, A theory of high-frequency distortion in bipolar transistors, IEEE Trans. Electron Devices 21 (1974) 745.
[27] S. Kim, B. Fisher, H.J. Eisler, M. Bawendi, Type-II quantum dots: CdTe/CdSe(Core/Shell) and CdSe/ZnTe(Core/Shell) heterostructures, J. Am. Chem. Soc. 125 (2003) 11466–11467.
[28] P.T.K. Chin, C. de Mello Doneg, S.S. van Bavel, S.C.J. Meskers, N.A.J.M. Sommerdijk, R.A.J. Janssen, Highly luminescent CdTe/CdSe colloidal heteronanocrystals with temperature-dependent emission color, J. Am. Chem. Soc. 129 (2007) 14880–14886.
[29] M.C. Troparevsky, Franceschetti, Radiative recombination of charged excitons and multiexcitons in CdSe quantum dots, Appl. Phys. Lett. 87 (2005) 263115–263117.